

# Surface operator content of the $A_L$ face models

Murray T. Batchelor<sup>1</sup>

*Department of Mathematics, School of Mathematical Sciences,  
The Australian National University, Canberra ACT 0200, Australia*

---

## Abstract

A set of fixed boundary weights for both the critical dense and dilute  $A_L$  face models is constructed from the known boundary weights of the related loop model. The surface operator content and the conformal partition functions then follow from the results obtained via the Bethe equations.

---

## 1 Introduction

The remarkable interplay between critical systems and the symmetries of conformal and modular invariance has been well illustrated by direct calculations on exactly solved models [1–3]. One well known family of such are the critical  $A$ - $D$ - $E$  models which are built from the Dynkin diagrams of the simply laced  $A$ - $D$ - $E$  Lie algebras [4]. These models can all be mapped onto an underlying loop model [4,5]. Another family of critical models, the dilute  $A$ - $D$ - $E$  lattice models [6–8], can be mapped onto the dilute  $O(n)$  loop model [9,10]. The bulk operator content and the modular invariant partition functions of these models are now well understood (see, e.g., [11]). However, the situation is not so clear for the surface operator content, at least from the perspective of exactly solved models.

The particular geometry of interest here is that shown in Fig. 1. We confine our attention to the  $A_L$  models. To distinguish between the two families, we refer to them as the dense  $A_L$  and the dilute  $A_L$  models, the nomenclature arising naturally from the corresponding loop models.

---

<sup>1</sup> Supported by the Australian Research Council

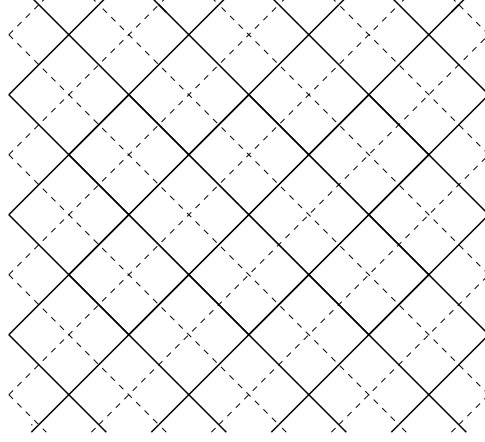


Fig. 1. An open square lattice in the vertical strip geometry. The face models under consideration are defined on the solid lines. The underlying loop and vertex models are defined on the dashed lines.

### 1.1 Face models

The bulk face weights of the dense  $A_L$  models at criticality are [4,12]

$$W \begin{pmatrix} c & \\ d & b \\ a & \end{pmatrix} = \rho_8(u) \delta_{a,c} A_{a,b} A_{a,d} + \sqrt{\frac{S_a S_c}{S_b S_d}} \rho_9(u) \delta_{b,d} A_{a,b} A_{b,c} \quad (1.1)$$

where

$$\rho_8(u) = 1, \quad \rho_9 = \frac{\sin u}{\sin(\lambda - u)} \quad (1.2)$$

and  $S_a = \sin a\lambda$ . The variable  $u$  is the spectral parameter and  $\lambda = \pi/h$  is the crossing parameter with Coxeter number  $h = L + 1$ . We are interested here in the boundary between regimes III and IV for which  $0 < u < \lambda$ . The elements of the adjacency matrix  $A$  are given by

$$A_{a,b} = \begin{cases} 1, & b = a \pm 1, \\ 0, & \text{otherwise.} \end{cases} \quad (1.3)$$

The bulk face weights of the dilute  $A_L$  models at criticality are [6–8]

$$\begin{aligned} W \begin{pmatrix} c & \\ d & b \\ a & \end{pmatrix} &= \rho_1(u) \delta_{a,b,c,d} + \rho_2(u) \delta_{a,b,c} A_{a,d} + \rho_3(u) \delta_{a,c,d} A_{a,b} \\ &+ \sqrt{\frac{S_a}{S_b}} \rho_4(u) \delta_{b,c,d} A_{a,b} + \sqrt{\frac{S_c}{S_a}} \rho_5(u) \delta_{a,b,d} A_{a,c} + \rho_6(u) \delta_{a,b} \delta_{c,d} A_{a,c} \end{aligned} \quad (1.4)$$

$$+ \rho_7(u)\delta_{a,d}\delta_{c,b}A_{a,b} + \rho_8(u)\delta_{a,c}A_{a,b}A_{a,d} + \sqrt{\frac{S_a S_c}{S_b S_d}} \rho_9(u)\delta_{b,d}A_{a,b}A_{b,c}$$

in which

$$\begin{aligned} \rho_1(u) &= 1 + \frac{\sin u \sin(3\lambda - u)}{\sin 2\lambda \sin 3\lambda} \\ \rho_2(u) = \rho_3(u) &= \frac{\sin(3\lambda - u)}{\sin 3\lambda} \\ \rho_4(u) = \rho_5(u) &= \frac{\sin u}{\sin 3\lambda} \\ \rho_6(u) = \rho_7(u) &= \frac{\sin u \sin(3\lambda - u)}{\sin 2\lambda \sin 3\lambda} \\ \rho_8(u) &= \frac{\sin(2\lambda - u) \sin(3\lambda - u)}{\sin 2\lambda \sin 3\lambda} \\ \rho_9(u) &= -\frac{\sin u \sin(\lambda - u)}{\sin 2\lambda \sin 3\lambda} \end{aligned} \tag{1.5}$$

and the generalised Kronecker delta is unity if all its arguments take the same value and zero otherwise. For these models

$$A_{a,b} = \begin{cases} 1, & b = a \text{ or } a \pm 1, \\ 0, & \text{otherwise.} \end{cases} \tag{1.6}$$

The regimes of interest here are

$$\begin{array}{lll} \text{regime 1} & 0 < u < 3\lambda & \lambda = \frac{\pi}{4} \frac{L}{L+1} \quad L = 2, 3, \dots \\ \text{regime 2} & 0 < u < 3\lambda & \lambda = \frac{\pi}{4} \frac{L+2}{L+1} \quad L = 3, 4, \dots \end{array}$$

where

$$h = \begin{cases} L + 2, & \text{regime 1,} \\ L + 1, & \text{regime 2.} \end{cases} \tag{1.7}$$

## 1.2 Loop models

To obtain a set of integrable boundary weights for the face models we consider the corresponding loop models, which have been solved in the open geometry of Fig. 1 [13,14]. The partition function of the dense  $O(n)$  loop model on the dashed lattice of Fig. 1 is defined by

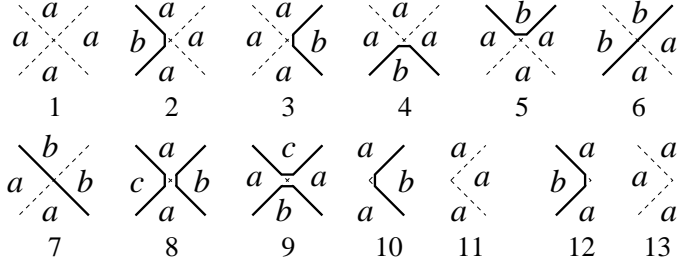


Fig. 2. The allowed vertices of the loop model along with the possible height configurations.

$$Z = \sum_{\mathcal{G}} \rho_8^{m_8} \rho_9^{m_9} \rho_{10}^{m_{10}} \rho_{12}^{m_{12}} n^P, \quad (1.8)$$

where the bulk weights  $\rho_8$  and  $\rho_9$  are given in (1.2). The sum is over all configurations  $\mathcal{G}$  of non-intersecting closed loops covering all lattice bonds. The two possible loop configurations at a vertex are numbers 8 and 9 in Fig. 2. In configuration  $\mathcal{G}$ ,  $m_i$  is the number of occurrences of the vertex of type  $i$ , while  $P$  is the total number of closed loops of fugacity  $n = 2 \cos \lambda$ . The boundary weights are

$$\rho_{10} = \rho_{12} = 1. \quad (1.9)$$

The partition function of the dilute  $O(n)$  model is defined by

$$Z = \sum_{\mathcal{G}} \rho_1^{m_1} \cdots \rho_{13}^{m_{13}} n^P, \quad (1.10)$$

where now the loops need not cover all lattice bonds and the loop fugacity is given by  $n = -2 \cos 4\lambda$ . The possible loop configurations at a vertex are shown in Fig. 2, with a vertex of type  $i$  carrying a Boltzmann weight  $\rho_i$ . The bulk weights are as given in (1.5). The integrable boundary weights are

$$\begin{aligned} \rho_{10} = \rho_{12} &= \sin\left[\frac{1}{2}(3\lambda - u) + \epsilon\right], \\ \rho_{11} = \rho_{13} &= \sin\left[\frac{1}{2}(3\lambda + u) + \epsilon\right]. \end{aligned} \quad (1.11)$$

There is one set for  $\epsilon = 0$ , the other for  $\epsilon = \frac{\pi}{2}$ .

Note that just as there is a loop formulation of the Yang-Baxter equation, ensuring integrability of the loop model in the bulk [15], there is also a loop formulation of the reflection equations, ensuring integrability at a boundary [16]. Rather than seeking explicit solutions of these equations our approach here is via the loop-to-face correspondence.

## 2 Boundary face weights and exact solutions

The face model transfer matrix  $\mathbf{t}_D(u)$  acts between three diagonal rows of the lattice, labelled by the heights  $\{a_0, a_1, \dots, a_N\}$ ,  $\{b_0, b_1, \dots, b_N\}$  and  $\{c_0, c_1, \dots, c_N\}$ , with  $a_{2k} = b_{2k}$  and  $b_{2k-1} = c_{2k-1}$ . Here  $N$  is the number of bulk edges in a row, which we take to be even. Thus

$$\begin{aligned} \mathbf{t}_D(u) = & K_+ \begin{pmatrix} c_0 & b_1 \\ b_0 & \end{pmatrix} \prod_{k=1}^{N/2-1} W \begin{pmatrix} & b_{2k-1} \\ a_{2k-2} & a_{2k} \\ & a_{2k-1} \end{pmatrix} W \begin{pmatrix} c_{2k} & \\ b_{2k-1} & b_{2k+1} \\ & b_{2k} \end{pmatrix} \\ & \times W \begin{pmatrix} & b_{N-1} \\ a_{N-2} & a_N \\ & a_{N-1} \end{pmatrix} K_- \begin{pmatrix} b_{N-1} & c_N \\ & b_N \end{pmatrix}. \end{aligned} \quad (2.1)$$

The bulk face weights of the  $A_L$  models are as given in (1.1) and (1.4). Now consider the boundary face weights.

### 2.1 Dense $A_L$ model

In accord with Fig. 2 we define the boundary face weights of the dense  $A_L$  model to be

$$K_+ \begin{pmatrix} a & \\ & a \pm 1 \end{pmatrix} = \rho_{10}, \quad K_- \begin{pmatrix} a \pm 1 & a \\ & a \end{pmatrix} = \rho_{12}, \quad (2.2)$$

where  $\rho_{10}$  and  $\rho_{12}$  may be arbitrary height-independent functions. General boundary face weights for this model have been discussed in [17,18].

The diagonal-to-diagonal transfer matrix  $\mathbf{t}_D(u)$  for the underlying loop model has eigenvalues [13,14]

$$\Lambda(u) = \rho_{10} \rho_{12} \prod_{j=1}^m \frac{\sinh[u_j + \frac{1}{2}i(u + \lambda)] \sinh[u_j - \frac{1}{2}i(u + \lambda)]}{\sinh[u_j + \frac{1}{2}i(u - \lambda)] \sinh[u_j - \frac{1}{2}i(u - \lambda)]}, \quad (2.3)$$

where  $u_j$  ( $j = 1, 2, \dots, m$ ) are roots of the Bethe equations

$$\begin{aligned} & \left[ \frac{\sinh[u_j + \frac{1}{2}i(u - \lambda)] \sinh[u_j - \frac{1}{2}i(u + \lambda)]}{\sinh[u_j + \frac{1}{2}i(u + \lambda)] \sinh[u_j - \frac{1}{2}i(u - \lambda)]} \right]^N \\ & = \prod_{\substack{k=1 \\ k \neq j}}^m \frac{\sinh(u_k + u_j - i\lambda) \sinh(u_k - u_j - i\lambda)}{\sinh(u_k + u_j + i\lambda) \sinh(u_k - u_j + i\lambda)}. \end{aligned} \quad (2.4)$$

## 2.2 Dilute $A_L$ model

Again in accord with Fig. 2 we define the boundary face weights of the dilute  $A_L$  model to be

$$\begin{aligned} K_+ \begin{pmatrix} a & \\ a & a \pm 1 \end{pmatrix} &= \rho_{10}, & K_+ \begin{pmatrix} a & \\ a & a \end{pmatrix} &= \rho_{11}, \\ K_- \begin{pmatrix} a & \\ a \pm 1 & a \end{pmatrix} &= \rho_{12}, & K_- \begin{pmatrix} a & \\ a & a \end{pmatrix} &= \rho_{13}, \end{aligned} \quad (2.5)$$

where the functions  $\rho_{10}$ – $\rho_{13}$  are as given in (1.11). The origin of the  $\epsilon$  factor is seen to be the double periodicity of the more general elliptic boundary weights [19].

With the given normalisation of the weights, the eigenvalues are [14]

$$\Lambda_D(u) = \rho_8^{N-1} \rho_{10} \rho_{12} \prod_{j=1}^m \frac{\sinh(u_j + i\lambda + \frac{1}{2}iu) \sinh(u_j - i\lambda - \frac{1}{2}iu)}{\sinh(u_j - i\lambda + \frac{1}{2}iu) \sinh(u_j + i\lambda - \frac{1}{2}iu)} \quad (2.6)$$

where the  $m$  roots  $u_j$  satisfy

$$\begin{aligned} \left[ \frac{\sinh(u_j - \frac{1}{2}i\lambda + i\epsilon)}{\sinh(u_j + \frac{1}{2}i\lambda + i\epsilon)} \right]^2 & \left[ \frac{\sinh(u_j - i\lambda - \frac{1}{2}iu) \sinh(u_j - i\lambda + \frac{1}{2}iu)}{\sinh(u_j + i\lambda - \frac{1}{2}iu) \sinh(u_j + i\lambda + \frac{1}{2}iu)} \right]^N \\ &= \prod_{\substack{k=1 \\ \neq j}}^m \frac{\sinh(u_j + u_k - 2i\lambda) \sinh(u_j - u_k - 2i\lambda)}{\sinh(u_j + u_k + 2i\lambda) \sinh(u_j - u_k + 2i\lambda)} \\ & \quad \times \frac{\sinh(u_j + u_k + i\lambda) \sinh(u_j - u_k + i\lambda)}{\sinh(u_j + u_k - i\lambda) \sinh(u_j - u_k - i\lambda)}. \end{aligned} \quad (2.7)$$

with again  $\epsilon = 0$  or  $\frac{\pi}{2}$ , depending on the choice of boundary weights.

## 3 Surface operator content

Let  $\Lambda_0$  be the largest eigenvalue of the transfer matrix. From the explicit calculations on the loop models, we know that the reduced free energy,  $f_N = -N^{-1} \log \Lambda_0$ , scales as

$$f_N = f_\infty + \frac{f_+}{N} + \frac{f_-}{N} - \frac{\pi\zeta c}{24N^2} + o(N^{-2}). \quad (3.1)$$

Here  $f_\infty$  is the bulk free energy,  $f_\pm$  are surface free energies and  $\zeta$  is a geometric factor. The rest of the eigenspectrum scales as

$$\log \frac{\Lambda_0}{\Lambda_\ell} = \frac{\pi\zeta(x_\ell + j)}{N} + o(N^{-1}), \quad (3.2)$$

where  $j = 0, 1, \dots$  defines the conformal tower of eigenstates associated with each eigenvalue. Both (3.1) and (3.2) are in agreement with the expectation from conformal invariance [1–3]. The quantities  $f_\infty$  and  $f_\pm$  are non-universal. Our interest here is in the universal scaling part of the spectrum defined by the central charge  $c$  and the surface scaling dimensions  $x_\ell$ . Their values can be inferred from the underlying loop models.

### 3.1 Dense $A_L$ model

Given the above boundary weights, a comparison of the finite-size transfer matrix eigenspectra of the dense  $A_L$  model on the one hand, and the dense  $O(n)$  loop model on the other, reveals a selection rule on the parameter  $m$  appearing in the Bethe equations (2.4). This parameter labels the sectors of the transfer matrix of the vertex model representation of the loop model. The restriction on  $m$  arises from the mapping of height configurations to arrow configurations on the underlying vertex model. Specifically,  $m = \frac{1}{2}N - \ell$ , for  $\ell = 0, 1, \dots, \ell_{\max}$ , where  $\ell_{\max} = \lfloor \frac{1}{2}(L - 1) \rfloor$ , the integer part of  $\frac{1}{2}(L - 1)$ . We confirm numerically that the eigenspectrum of the face model is exactly equivalent to the eigenspectrum of the loop model with the above restriction. However, the equivalence is not one-to-one, as the degeneracies differ. For example, the largest eigenvalue is  $L$ -fold degenerate in the face model. There are eigenstates in the  $\ell \leq \ell_{\max}$  sectors of the loop model which are not eigenstates of the face model. However, these are precisely the same eigenvalues which appear in the sectors with  $\ell > \ell_{\max}$ . As a result the surface operator content of the face model can be inferred from the known results for the loop model.

The central charge and surface scaling dimensions of the loop model are [13,20,21]

$$c = 1 - \frac{6\lambda^2}{\pi(\pi - \lambda)}, \quad x_\ell = \frac{\ell}{\pi}[\ell(\pi - \lambda) - \lambda], \quad (3.3)$$

where  $\ell$  is unrestricted. The Bethe equation calculations also reveal a set of constant scaling dimensions, with  $x = 2$ . Now consider the face model. In

terms of the Kac formula [1–3]

$$\Delta_{r,s} = \frac{[hr - (h-1)s]^2 - 1}{4h(h-1)} \quad (3.4)$$

we have, recalling that  $\lambda = \pi/h$  with  $h = L + 1$ ,

$$c = 1 - \frac{6}{h(h-1)}, \quad (3.5)$$

$$x_\ell = \Delta_{1,1+2\ell}, \quad \ell = 1, \dots, \lfloor \frac{1}{2}(h-2) \rfloor. \quad (3.6)$$

Along with the constant dimension  $x = 2$ , this defines the surface operator content of the dense  $A_L$  face model.

The first example is the Ising model with  $h = 4$ ,  $c = \frac{1}{2}$ ,  $x_\sigma = \frac{1}{2}$  and  $x_\epsilon = 2$ . The next few cases are  $h = 5$ , with  $c = \frac{7}{10}$ ,  $x = \frac{3}{5}$ ,  $x = 2$ , and  $h = 6$ ,  $c = \frac{4}{5}$ ,  $x = \frac{2}{3}$ ,  $x = 2$ ,  $x = 3$ . Recall that the boundary heights are fixed along each boundary, but free to take all allowed values. The operator content induced by other boundary configurations and different geometries have also been considered for this particular family of models [20,22–24].

The modular invariant partition functions can be constructed from the central charge and conformal dimensions through the Virasoro characters [1–3]

$$\begin{aligned} \chi_{r,s} &= \frac{q^{-\frac{c}{24} + \Delta_{r,s}}}{Q(q)} \sum_{n=-\infty}^{\infty} q^{n^2 h(h-1) + nhr} \left[ q^{-n(h-1)s} - q^{n(h-1)s+rs} \right], \\ &= q^{-\frac{c}{24} + \Delta_{r,s}} \sum_{n=0}^{\infty} d_n(\Delta_{r,s}) q^n, \end{aligned} \quad (3.7)$$

where

$$Q(q) = \prod_{n=1}^{\infty} (1 - q^n). \quad (3.8)$$

The first few integer co-efficients  $d_n(\Delta_{r,s})$  are tabulated in, e.g., [3]. From the face model eigenspectra we see that the first few modular invariant partition functions for the fixed boundaries under consideration are

$$\begin{aligned} h = 4, \quad Z &= 3\chi_{1,1} + 3\chi_{1,3}, \\ h = 5, \quad Z &= 4\chi_{1,1} + 6\chi_{1,3}, \\ h = 6, \quad Z &= 5\chi_{1,1} + 9\chi_{1,3} + 5\chi_{1,5}. \end{aligned} \quad (3.9)$$



We can add  $h = 3, Z = 2\chi_{1,1}$  [20] to begin this list. These relations define the asymptotic degeneracies of the eigenspectrum.

### 3.2 Dilute $A_L$ model

The transfer matrix eigenspectrum of the dilute  $A_L$  face model is equivalent to that of the dilute loop model with the restriction  $m = N - \ell$ , where  $\ell = 0, 1, \dots, \ell_{\max}$ , with  $\ell_{\max} = L - 1$ . Again it is precisely the eigenvalues in the  $\ell > \ell_{\max}$  sectors which do not appear in the eigenspectrum of the face model.

The central charge and surface scaling dimensions of the dilute  $O(n)$  model with boundary weights (1.11) have been calculated from the exact solution of section 2.2 at the particular value  $u = \lambda$  [25–28]. This is the so-called honeycomb limit of relevance to the surface critical behaviour of self-avoiding random walks [29,26,27,30]. It is straightforward to extend these calculations to the wider range  $0 < u < 3\lambda$ . Indeed, the central charge and scaling dimensions are independent of the spectral parameter  $u$ . The central charge is

$$c = 1 - 6(g - 1)^2/g, \quad (3.10)$$

where  $\pi g = 2\pi - 4\lambda$ . Three sets of “geometric” scaling dimensions have been derived, each corresponding to a choice of the boundary weights. For  $\epsilon = 0$ , the result is [29,25,28]

$$X_\ell^{\text{O-O}} = \frac{1}{4}g\ell^2 + \frac{1}{2}(g - 1)\ell. \quad (3.11)$$

In the language of surface critical phenomena, O–O labels the ordinary surface transition. The choice  $\epsilon = \frac{\pi}{2}$  (S–S) corresponds to the special surface transition. The other possibility is mixed O–S boundary conditions with  $\epsilon = 0$  on one side of the strip and  $\epsilon = \frac{\pi}{2}$  on the other, for which there is also a Bethe solution [27,28]. The extraordinary surface transition has also been recently discussed [31]. We confine our attention here to the O–O boundaries. The thermal dimension has also been calculated, with in this case  $x = 2$ .

For regime 1,  $g = \frac{h}{h-1}$  with  $h = L + 2$ . The central charge (3.10) gives the unitary minimal result (3.5). The scaling dimensions are given in terms of the Kac formula by

$$X_\ell^{\text{O-O}} = \Delta_{1+\ell,1}, \quad \ell = 1, \dots, h - 3. \quad (3.12)$$

As for the dense model, the Ising case has  $h = 4$  with  $c = \frac{1}{2}$ ,  $x_\sigma = \frac{1}{2}$  and  $x_\epsilon = 2$ .

The first few conformal partition functions are given by

$$\begin{aligned}
h = 4, \quad Z &= 2\chi_{1,1} + 2\chi_{2,1}, \\
h = 5, \quad Z &= 3\chi_{1,1} + 4\chi_{2,1} + 3\chi_{3,1}, \\
h = 6, \quad Z &= 4\chi_{1,1} + 6\chi_{2,1} + 6\chi_{3,1} + 4\chi_{4,1}.
\end{aligned} \tag{3.13}$$

Since  $\chi_{2,1} = \chi_{1,3}$  for  $h = 4$  both the dense and dilute results are essentially the same for the Ising case.

For regime 2,  $g = \frac{h-1}{h}$  with  $h = L + 1$ . The central charge is again given by (3.5) with scaling dimensions

$$X_\ell^{\text{O-O}} = \Delta_{1,1+\ell}, \quad \ell = 1, \dots, h - 2. \tag{3.14}$$

In this regime the Ising results for  $h = 4$  are  $c = \frac{1}{2}$ ,  $x = \frac{1}{16}$ ,  $x = \frac{1}{2}$  and  $x = 2$ . Here the first few conformal partition functions are given by

$$\begin{aligned}
h = 4, \quad Z &= 3\chi_{1,1} + 4\chi_{1,2} + 3\chi_{1,3}, \\
h = 5, \quad Z &= 4\chi_{1,1} + 6\chi_{1,2} + 6\chi_{1,3} + 4\chi_{1,4}, \\
h = 6, \quad Z &= 5\chi_{1,1} + 8\chi_{1,2} + 9\chi_{1,3} + 8\chi_{1,4} + 5\chi_{1,5},
\end{aligned} \tag{3.15}$$

again from which the general pattern is readily apparent.

## 4 Conclusion

A set of particular fixed boundary weights has been constructed for both the dense and dilute  $A_L$  face models from the boundary weights of the related loop model. The transfer matrix eigenspectra of the face models is seen to agree with that of the loop models under restriction of the parameter  $\ell$ . The surface operator content and the conformal partition functions then follow from the results obtained via the Bethe equations for the loop models. It will be particularly worthwhile to generalise these Bethe solutions in terms of the elliptic  $\vartheta$ -functions of the off-critical  $A_L$  models, as was done originally in the bulk [12,32].

## Acknowledgements

It is a great pleasure to wish Professor J.M.J. van Leeuwen all the best on this occasion. I look back fondly on my first postdoc, in Leiden, under his

inspirational guidance. Among other things, he taught me to take my first steps on the ice. This manuscript has benefited from helpful discussions with Katherine Seaton, Ole Warnaar and Yu-kui Zhou.

## References

- [1] C. Itzykson, H. Saleur and J.B. Zuber, eds., *Conformal invariance and applications to statistical mechanics* (World Scientific, Singapore, 1988).
- [2] J.L. Cardy, ed., *Finite-size scaling* (North-Holland, Amsterdam, 1988).
- [3] P. Christe and M. Henkel, *Introduction to conformal invariance and its applications to critical phenomena*, (Springer, Heidelberg, 1993).
- [4] V. Pasquier, Nucl. Phys. B 285 (1987) 162; J. Phys. A 20 (1987) L1229.
- [5] A.L. Owczarek and R.J. Baxter, J. Stat. Phys. 49 (1989) 1093.
- [6] S.O. Warnaar, B. Nienhuis and K.A. Seaton, Phys. Rev. Lett. 69 (1992) 710.
- [7] Ph. Roche, Phys. Lett. B 285 (1992) 49.
- [8] S.O. Warnaar, B. Nienhuis and K.A. Seaton, Int. J. Mod. Phys. B 7 (1993) 3727.
- [9] B. Nienhuis, Int. J. Mod. Phys. B 4 (1990) 929.
- [10] S.O. Warnaar and B. Nienhuis, J. Phys. A 26 (1993) 2301.
- [11] D.L. O'Brien and P.A. Pearce, J. Phys. A 28 (1995) 4891.
- [12] G.E. Andrews, R.J. Baxter and P.J. Forrester, J. Stat. Phys. 35 (1984) 193.
- [13] A.L. Owczarek and R.J. Baxter, J. Phys. A 22 (1989) 1141.
- [14] C.M. Yung and M.T. Batchelor, Nucl. Phys. B 435 (1995) 430.
- [15] S.O. Warnaar, B. Nienhuis and H.W.J. Blöte, J. Phys. A 26 (1993) 477.
- [16] M.T. Batchelor, unpublished.
- [17] R.E. Behrend, P.A. Pearce and D.L. O'Brien, J. Stat. Phys. 84 (1996) 1.
- [18] C. Ahn and W.M. Koo, Nucl. Phys. B 468 (1996) 461.
- [19] M.T. Batchelor, V. Fridkin and Y.K. Zhou, J. Phys. A 29 (1996) L61.
- [20] H. Saleur and M. Bauer, Nucl. Phys. B 320 (1989) 591.
- [21] M.T. Batchelor, A.L. Owczarek, K.A. Seaton and C.M. Yung, J. Phys. A 28 (1995) 839.
- [22] J.L. Cardy, Nucl. Phys. B 324 (1989) 581.

- [23] L. Chim, Int. J. Mod. Phys. A 11 (1996) 4491.
- [24] P.A. Pearce, unpublished.
- [25] M.T. Batchelor and J. Suzuki, J. Phys. A 26 (1993) L729.
- [26] M.T. Batchelor and C.M. Yung, Phys. Rev. Lett. 74 (1995) 2026.
- [27] M.T. Batchelor and C.M. Yung, J. Phys. A 28 (1995) L421.
- [28] C.M. Yung and M.T. Batchelor, Nucl. Phys. B 453 (1995) 552.
- [29] B. Duplantier and H. Saleur, Phys. Rev. Lett. 59 (1987) 539.
- [30] D. Bennett-Wood and A.L. Owczarek, J. Phys. A 29 (1996) 4755.
- [31] M.T. Batchelor and J. Cardy, Extraordinary transition in the two-dimensional  $O(n)$  model, cond-mat/9705238
- [32] V.V. Bazhanov, B. Nienhuis and S.O. Warnaar, Phys. Lett. B 322 (1994) 198.